

Eco-friendly filtration of Nickel from the sludge during electrochemical machining of Monel 400 alloys

Vengatajalapathi N.^{1*}, Ayyappan S.¹ and Rajasekar V.¹

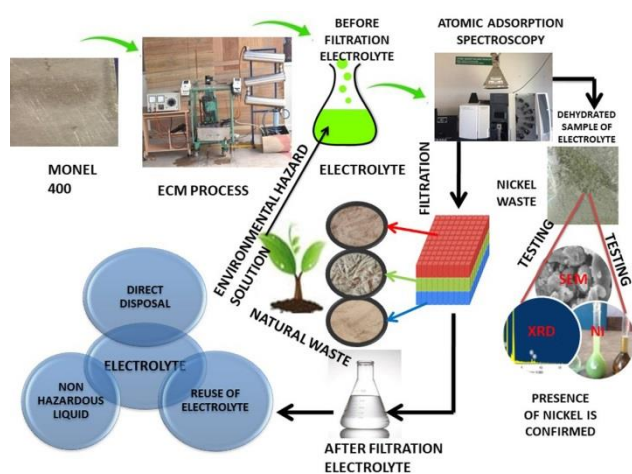
¹Government College of Technology, Coimbatore- 641013, Tamil Nadu, India

Received: 13/12/2021, Accepted: 09/02/2022, Available online: 17/02/2022

*to whom all correspondence should be addressed: e-mail: vengat92vengat@gmail.com

<https://doi.org/10.30955/gnj.004226>

Graphical abstract



Abstract

Electrochemical Machining played a vital role in the aircraft, atomic, and healthcare industries via electrochemical machining (ECM). Even with difficult-to-machine materials. ECM has generally preferred to machine Nickel-based alloys compared to other non-conventional and conventional machining tools. During machining with ECM, the Nickel-based alloys discharge toxic nickel hydroxides in sludge, which is very harmful to the environment. Therefore, in this work, investigations have been made to analyze the amount of nickel content discharges into the electrolyte and develop an eco-friendly filtering mechanism for nickel discharges to attain sustainable manufacturing. Bio-degradable coconut shell powder and wood dust powder were used in the filtration set up to filter the sludge. Thus, Eco-Friendly Electrochemical Machining (EECM) was developed and investigated the machining on Monel 400 alloys. Measurements including applied voltage (V), flow rate (U), and electrolyte concentration were commonly used to compare the amount of material removal rate (MRR) and the amount of nickel in the electrolyte before and after filtering. The contour plots were designed to show the impact of cycle boundaries on nickel particle releases and their collaboration. Researchers found that natural environmental debris, including coconut shell powder,

wood dust powder, and bagasse, were excellent at filtering out nickel levels from the electrolyte.

Keywords: Eco-friendly Electrochemical Machining (EECM), Material Removal Rate (MRR), Environmental pollutants, Monel400 combination alloys.

1. Introduction

The automobile industry is one of the most rapidly expanding sectors of the global economy. Hard-to-machine materials like instrument steel, carbides, and superalloys like titanium alloys are used in this field. As a result of the unique benefits it offers, electrochemical machining (ECM) has sparked the interest of the mechanical community in recent decades. These benefits include lower instrument wear, reduced mechanical power consumption, and no heat-influenced zones. Electro-Chemical Machining (ECM) is superior to electroplating when machining hard materials or complex forms. Using a mold to apply pressure to electrically conductive materials, electrochemical disintegration is a nuclear-level anodic process that is controlled. During electrochemical machining (ECM), the workpiece is the anode, the equipment is the cathode, and the electrolyte is pumped through the IEG between the two. This electrochemical circuit may be saturated with a lot of current to break up metal from the workpiece into metal hydroxides. Particle growth sends electrons on a path that's completely against the flow of positive energy. Faraday's law states that the quantity of metal destroyed in a circuit is exactly proportional to the amount of current flowing. The industrial usage of ECM and hybrid methods has grown in recent years. Precision and accuracy are required in machining. Thus the electronics industry uses ECM to make its tiny parts. Despite these advancements, more study is needed in ECM, particularly in tool design, measure control, and electrolyte management. ECM is primarily used for the machining of extremely hard superalloys, particularly nickel-based alloys (Xu and Wang, 2019). ECM is a very efficient and low-cost machining technique for Ni-based alloys the electrochemical dissolution behavior of a Ni-based superalloy was studied using nano3 electrolyte (Yong Cheng *et al.* (2017). Tools are the focus of the ECM

process for Ni-based alloys. Tools are the focus of the ECM process for Ni-based alloys (Burger *et al.*, 2012). ECM conducted several studies on the machinability of Ni alloys (Curtis *et al.*, 2009; Xiaolei *et al.*, 2020; Yong Cheng *et al.*, 2019; Zhang *et al.*, 2016). Aircraft, rocket engines, power generation turbines, chemical processing plants, and nuclear power plants are among the many applications for nickel alloys. There are several hazardous by-products generated during milling Ni-based alloys, such as Ni and Chromium hydroxides, as well as gaseous by-products such as acids, nitrates, and sulfates as well as oils and metal ions. Eyes and skin are irritated by electrolyte splashing, and a hazardous fume is allowed to grow unhindered. Sludge also significantly influences the current flow through the gap between the tool and the workpiece. The electrolyte and ECM slurry have the most impact on the environment. A requirement for high material removal rate (MRR) and surface finish urges to exercise quality electrolytic solutions ignoring its environmental impacts. When chrome metals dissolve in aqueous sodium nitrate (NaNO_3), toxic chromate, nitrate, and smelling ions accumulate in the sludge due to the nitrate decreasing at the tool cathode (Tonshoff *et al.*, 1996). When these disposals reach dangerously high levels, the live biological thing suffers. Despite their importance, heavy metals like cadmium, chromium, and nickel are often employed in industrial processes because they are hazardous to human health and the environment (Srivastava and Majumder, 2008). The preparation and removal of sludge containing hazardous materials are time-consuming and expensive. Repeated usage of the electrolyte may leave some of these harmful emissions in the electrolyte. It's possible, though, that using this technique would reduce machining performance. Chemically inert solids with no hazardous substance can be washed away before waste treatment. Liquids and oils that have not been emulsified are easy to separate. Emulsion breaking is used to remove liquid emulsions from electrolytes. Chemical-physical measures must be used to address electrolyte arrangements. If hazardous pollutants in the slurry are not removed before disposal, the soil will become polluted. Sludge containing chromium III compounds may oxidize to produce hazardous chemicals called soluble chromates. ECM's economic efficiency is boosted by detoxification and subsequent metal hydroxide deposition costs. When detoxifying chemicals are added during machining, sulfate ions are formed, causing process disruptions. In the aerospace and marine industries, materials based on nickel have great corrosion resistance. While sustaining productivity and quality, environmentally sustainable machining of Ni-based alloys in ECM is required (Watkins and Granoff, 1992). ECM's machining concept makes it simple to produce parts using Ni-based alloys. Even yet, a significant amount of Nickel ions are released into the electrolyte slurry throughout the process. Toxic effects on respiratory and excretory organs are possible if nickel levels are exceeded. The most persistent side effect of Ni exposure is dermatitis (Rajurkar, 1999). Nickel pollution in the environment is responsible for many diseases,

including diarrhea, pallor, renal damage, hepatitis, and central nervous system malfunctions. Human carcinogens, as well as few living organisms, cannot break down by metal ions. Catalyst activators and digestive responses benefit from low concentrations of Ni(II) molecules. Bureau of Indian Standards (BIS): IS 10500 specifies a nickel particle concentration limit of 0.02 mg/L in drinking water (2012). To prevent harm to the environment and human health, the effluent should be treated to eliminate the hazardous Ni heavy metal. As a result, ecologically responsible manufacturing has recently shifted its attention to ECM. Activated carbons, chemical precipitation, ion exchange, ion-flotation adsorption, layer filtration, and electrochemical processes are some treatment techniques utilised to remove Ni ions (Kumar, 2019). Agricultural waste products have been increasingly used as adsorbents in recent years since alternative treatment processes are expensive to regenerate. In the agro-waste products, the cellulose and lignin include the different functional groups, such as alcohols, carboxylic corrosive, ketones, and ether. When these functional groups are combined with significant metals, they can form complexes using an electron pair. Rural trash, rice husk is prosperous industries' by-product and includes a large quantity of floristic fiber, proteins and hydroxyl, carboxyl, and amidogen, functional groups. Adsorption is made more accessible by these components. To remove Ni(II) ions, rice bran combined with a few synthetic chemicals was used (Crini, 2006). Using genetically modified rice and hydrochloric acid-treated rice bran, Ni(II) metal particles from an aqueous solution were eluted from the solution (Zafar *et al.*, 2015). Using coir essence, a waste product from the coir industry can cure Ni(II) due to its high cellulose and lignin content (Ewecharoen *et al.*, 2008). The nickel plating industry's effluent was remedied using barley straw to remove Ni(II) metal particles (Thevannan *et al.*, 2010). Punica granatum strip waste was used to investigate nickel bio-sorption from an aqueous solution (Bhatnagar and Minocha, 2010). Ni(II) remediation from industrial wastewater has been tested using the Citrus Limettioides peel (Ajmal *et al.*, 2000; Sudha *et al.*, 2015). Different adsorption limits, such as pH, temperature, contact duration, and adsorbent percentage, focused the nickel particle adsorption conductivity on Cashew nutshell (Kumar *et al.*, 2011). Industrial effluent Ni(II) metal particles were adsorbed on Quercus ithaburensis waste oak seed (Malkoc *et al.*, 2010). Oak (Quercus coccifera) sawdust was used to study the heavy metal ion (Cu, Ni, and Cr) adsorption from an aqueous bath and the optimal adsorption process parameters, i.e. shaking speed, adsorption mass, and pH, were found (Argun *et al.*, 2007). Using rice husk, Ni metal ions from industrial wastewater may be remedied because of their high adsorption characteristics (Ajmal *et al.*, 2003). Other adsorption study materials shown to be effective in removing Ni ions were orange peels, black carrot, almond husk, mosambi fruit peelings, tea trash, and peepal leaves (Gönen and Serin, 2012). According to the cited literature, various agro-wastes have been tested for nickel ion removal from

aqueous solutions, and they all worked. Prevention of front-end pollution, i.e. elimination of hazardous element production during machining, is problematic in ECM. As a result, treatment and disposal at the "end of the pipe" are being employed in this research. Using bio-wastes as adsorbents for nickel ions from sludge when milling nickel-based Monel 400 alloys by ECM, this approach utilized coconut shell powder, waste wood dust, and Bagasse.

2. Experimentation

Monel 400, a readily available nickel-based alloy, was used in this investigation as a test sample. Table 1 shows the Monel 400 composites' synthetic structure.

Eco-friendly Electrochemical Machining (EECM) setup was developed for this study. The schematic diagram of EECM is displayed in Figure 1. EECM contains a power supply framework, electrolyte supply framework, filtering

Table 1. Chemical composition of Monel 400alloys

Composition and weight(%)	Monel 400alloys								
	C	Si	Mn	P	S	Cr	Mo	Fe	V
	0.047	0.172	1.03	0.012	0.01	0.1	0.1	1.66	0.029
	W	Cu	Al	Co	Nb	Ti	Mg	Ni	
	0.1	29.24	0.01	0.103	0.1	0.047	0.031	67.4	

Table 2. Factors and state of ECM Experiments are arranged

Factors	Type	Condition/size
WorkPiece	Monel 400alloys	Toughenedmaterial
Electrolyte	Sodium chloride	130-190g/L
Tool	Copper	C101
Voltage	DC	11,13,15 V
Tool feedrate	Horizontalfeed	0.1mm/min
Inter-electrode gap		0.1mm
Current	DC	50A
Flowrate		1-3L/min
Machining time		5 min

Table 3. Process parameters and levels

S.No.	Process parameters	Levels				
		-2	-1	0	1	2
1	Voltage(V)	11	12	13	14	15
2	ElectrolyteConcentration(g/L)	130	145	160	175	190
3	Flowrate(L/min)	1	1.5	2	2.5	3

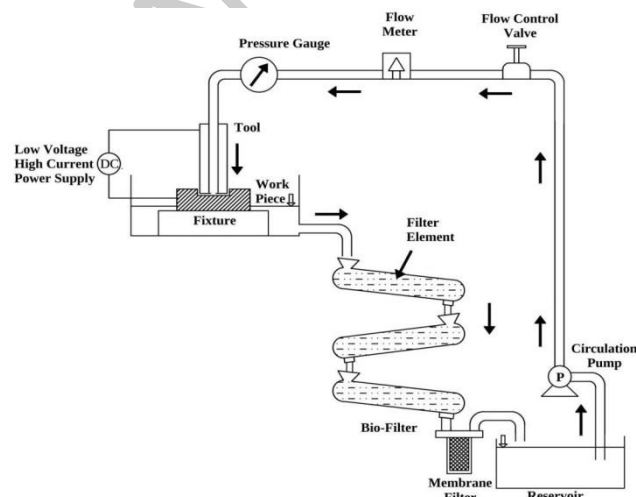


Figure 1. Schematic diagram of the filtration setup.

system, tool feed mechanism, work holding and position system, control panel, and edge. The electrolyte (for example, NaCl watery arrangement) flows at a high rate (1-10 L/min) through the Inter electrode terminal hole (0.1-0.6 mm). An 11-15V direct current (DC) potential with a current density of 20 to 110 A/cm² is applied across the Inter-Electrode Gap (IEG) between a copper tool and an anode workpiece. At low current densities, the MRR is low. The higher current densities of 110 A/cm² are utilized to have high current efficiency. The anodic disintegration rate, represented by Faraday's laws of electrolysis, depends upon the electrochemical properties of the metal, the electrolyte properties, and the current/voltage provided. The device is fed against the workpiece, which is immovably fixed on the fixture. IEG, adequate voltage (V), and current (I) are set in the control board. The filtration system consists of compartments for holding the bio-absorbents and membrane filter.

The copper tool is used as an anode. The diameter and electrolyte exit hole of the tool is 8mm and 2mm, respectively. MRR is straightforwardly proportionate to the feed pace of the apparatus [30]. When the applied voltage is high, the machining current is expanded to bring about high MRR. Low voltage brings about poor machining execution [31]. The voltage scope of 11–16 V was considered in some such examinations in ECM to have better performance as far as MRR and surface completion [32, 33]. In this manner, the voltage range (10–15 V) accessible in the arrangement is utilized for this examination. High focus diminishes the portability of particles which brings about poor anodic disintegration. The fixation levels in the scope of around 100 g/L to 200 g/L impacts the MRR essentially [31]. The primary interaction boundaries administering the ECM considered

are voltage (V), flow rate, and EC as indicated by the writing. Accordingly, these parameters are considered in this examination, and their levels are displayed in Table 2.

The IEG is set to 0.1mm, and the current of 50A is given to the DC rectifier. The machining was accomplished for 5 min. The operating states of EECM are summed up in Table 2.

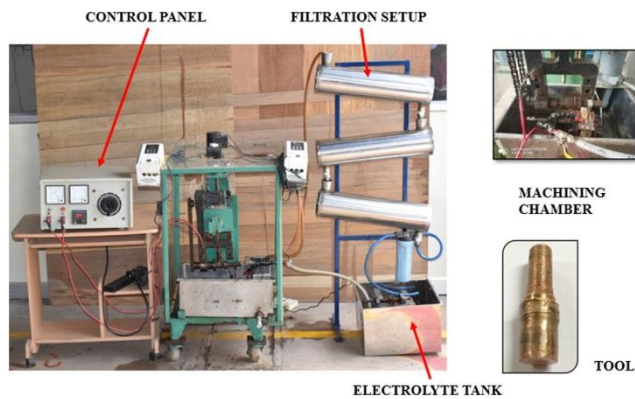


Figure 2. EECM experimental setup.

The central composite design (CCD) of response surface methodology (RSM) is taken on with the software Minitab-17 for the process parameters, and its levels are displayed in Table 3. In this work, 20 tests were completed with different parameter combinations, as in Figure 3.

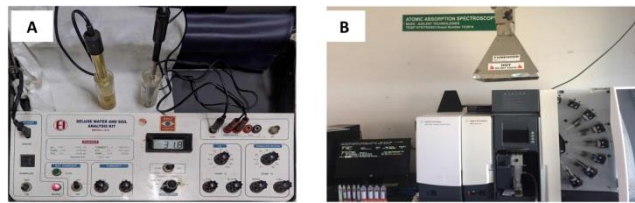


Figure 3. (a) Water analysis kit, (b) Atomic absorption spectroscopy.

The HCl concentration of 1% was added to the NaCl electrolyte to minimize the sludge formation in IEG. The electrolyte was pneumatically pumped from a stainless steel reservoir. The water analysis kit-191E (Environmental & Scientific Instruments Co.) as in Figure 4 was used to observe the electrolyte's pH, conductance, and temperature.

The sludge discharged after machining with ECM contains the nickel content for 250mg/L as tested by Atomic Absorption Spectroscopy (AAS) shown in Figure 3(b).

The green color of the sludge indicates the presence of nickel in the electrolyte, as shown in Figure 4(a). Further, the precipitate of electrolyte was tested in X-Ray powder Diffraction (XRD) and confirmed the presence of nickel. Figure 4(b) represents the XRD results of electrolyte sludge. The peaks in the figure confirm the presence of more nickel, chloride, and sodium particles.

The scanning electron microscopy (SEM) images of sludge as in Figure 4(c) show the significant presence of nickel. Cloudy spots on the image indicate the nickel elements.

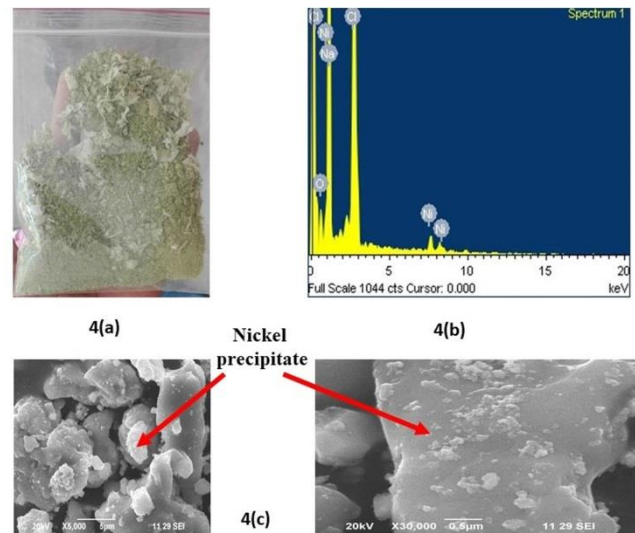


Figure 4. (a) Precipitate of the electrolyte solution of Monel400 (b) EDAX result of nickel in the precipitate (c) SEM image of sludge.

2.1. Mathematical modelling and analysis of variance

A second-order polynomial model, Eqn, was developed to examine the impact of ECM process parameters on the discharge of nickel elements into the electrolyte. (1).

$$\begin{aligned} \text{Ni(Pr)} = & 304.5254 - 0.04654 * \text{EC} - 37.6387 * \text{V} - \\ & 31.8736 * \text{U} + 1.50348 * \text{V}^2 + 4.2139 * \text{U}^2 \\ & + 0.13117 * \text{EC} * \text{U} \end{aligned}$$

ANOVA and Fisher's test (F-ratio) have been used to demonstrate the model's accuracy and efficacy. Values of "Prop > F" less than 0.05 indicate the model's and terms' meaning. When the value is larger than 0.1, the model terms are considered insignificant. According to Table 5, where the model's F-value is 24.41, the model is very significant. The model's terms are significant. The nickel presence model created shows adequate as a coefficient of determination (Coefficient of Regression). Values $R^2 = 0.9245$ and $R^2_{\text{adj}} = 0.881$ are significant. The normal probability curve in Figure 8 confirms the adequacy of the model equation.

2.2. Parametric influence on Ni presence

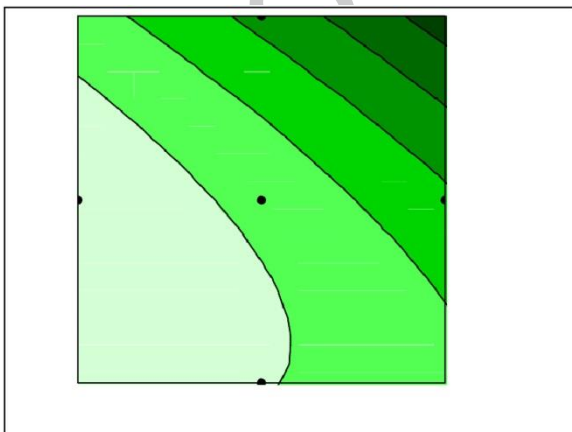
Figure 5 depicts the influence of cycle factors on the Nickel presence during the electrochemical Machining of Monel 400 compounds. The contour plot shows the impact of flow rate and electrolyte concentration on the discharge nickel components in the slime. It very well may be seen that the change in electrolyte concentration up to 160g/L to 190g/L gradually increases the sludge removal which contains the nickel elements. Higher concentration helps in increasing the speed of electrochemical responses and it brings about more removal. The flow rate above 1.5 L/min removes the sludge from the gap between tool and workpiece better to result in the fresh surface of the specimen for further electrochemical reaction. Higher flow rates increase the nickel ions in the electrolyte discharge. The machined specimen is shown in Figure 6.

Table 4. The trial results were seen as arranged

Exp.No.	EC (g/L)	V (V)	U (L/min)	Nipresence(mg/L)
1	190	13	2.0	65.00
2	160	13	2.0	57.20
3	145	12	2.5	58.00
4	175	14	2.5	67.45
5	160	13	2.0	55.64
6	130	13	2.0	50.64
7	160	13	1.0	55.40
8	160	13	2.0	56.45
9	175	12	1.5	58.60
10	160	11	2.0	57.40
11	160	13	2.0	56.40
12	160	13	3.0	66.50
13	145	12	1.5	55.24
14	145	14	2.5	60.08
15	160	13	2.0	55.40
16	175	14	1.5	58.24
17	160	15	2.0	68.10
18	145	14	1.5	54.00
19	160	13	2.0	58.00
20	175	12	2.5	66.10

Table 5. ANOVA results for the experimental data

Source	Sum of Squares	DF	Mean Square	F Value	P-value Prob > F	Significance
Regression	428.0772	6	71.3462	24.4096	< 0.0001	Significant
EC	167.6378	1	167.6378	57.3538	< 0.0001	
V	33.7271	1	33.7271	11.5390	0.0048	
U	142.5039	1	142.5039	48.7547	< 0.0001	
EC*U	7.7421	1	7.7421	2.6488	0.1276	
V^2	59.5697	1	59.5697	20.3805	0.0006	
U^2	29.2471	1	29.2471	10.0063	0.0075	
Residual	37.9973	13	2.9229			Not significant
Lack of Fit	33.2966	8	4.1621			
Pure Error	4.7008	5	0.9402	4.4270	0.0590	
Total	466.0745	19				

**Figure 5.** Contour plot of nickel presence (mg/L) vs U (L/min) and EC (g/L).

2.3. Adsorption of Ni ions

These environmental waste materials such as coconut shell powder, waste wood dust, and bagasse (Figure 7) were collected from various sources. Waste wood dust

was obtained with a sieve size of 40–50 mesh, washed with refined water, and dried in daylight for 2 hours. Grinded coconut shell to a fineness of 30-40 mesh. The nickel adsorption capacity of coir coconut powder is not affected by the particle size [35]. It was dried after being cleaned with distilled water and dried again. Bagasse washed with distilled water and dried in the open air before being used. Using coconut shell powder, bagasse, and waste wood dust as bio-adsorbents, the absorbent tubes of filtration were filled with the bio-adsorbents.

**Figure 6.** The machined specimen.

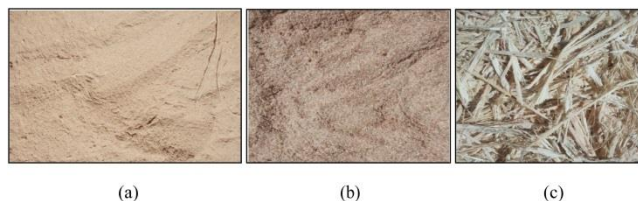


Figure 7. (a) Coconut shell powder, (b) Waste wood dust and (c) Bagasse.

The ECM sludge is exposed to the adsorbent materials for 20 minutes before being removed. AAS equipment was used to measure the amount of nickel in the electrolyte solution before and after filtering.

The ideal grouping of the stock arrangement of the sludge, ranging from 20–100 mg/L solution was prepared by dissolving in the ten times of distilled water. Otherwise high concentration solution in the testing leads to the quick failure of AAS equipment. The electrolytic solution was collected from each machining condition of ECM as in Table 4 and allowed to flow through the electrolyte filtration setup. The eco-friendly fibers in the filtration remove the nickel and the electrolyte became free of green colour as given in Figure 8. The green color is

created by the presence of nickel content in the electrolyte solution. The brown color of the treated solution is developed by the wood dust in the filtration.

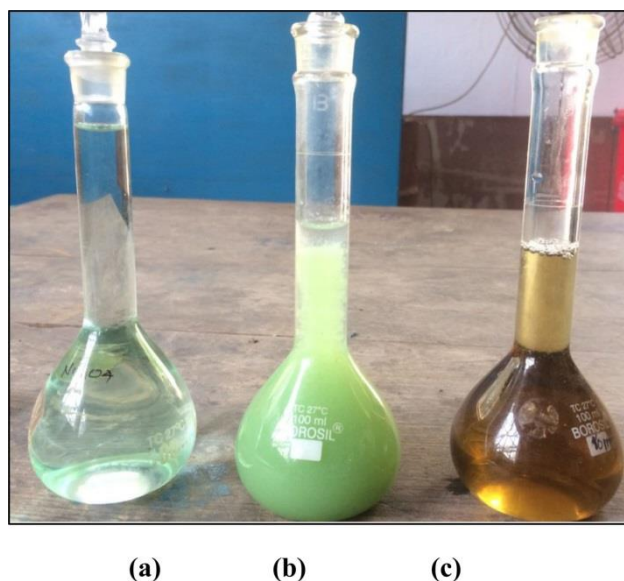


Figure 8. (a) Nickel standard solution (b) Solution before filtration (c) After filtration.

Table 6. Limits of process and performance parameters

Variable	Goal	Lower	Upper	Weight	Weight	Importance
EC	In the range	130	190	1	1	3
V	In the range	11	15	1	1	3
U	In the range	1	3	1	1	3
Ni presence	Minimize	50.64	68.1	1	1	3

Table 7 Optimization results

Solutions					
Number	EC	V	U	Ni presence	Desirability (Ni)
1	130	12.210	1.390	50.5976	1
2	130	12.490	1.370	50.5202	1
3	130	12.830	1.630	50.0980	1
4	130	12.890	1.440	50.5093	1
5	130	12.640	1.670	49.9318	1
6	130	12.160	1.720	50.0799	1
7	130	12.850	1.660	50.0892	1
8	130	12.220	1.990	50.2443	1
9	130	12.740	2.110	50.4790	1
10	130	13.090	1.780	50.3752	1
11	130	12.350	1.400	50.4749	1
12	130	12.860	1.490	50.3537	1
13	130	12.220	1.540	50.2202	1
14	130	12.890	1.960	50.2533	1
15	130	12.200	2.020	50.3274	1
16	130	12.535	1.768	49.8776	1
17	130	12.810	1.770	50.0023	1
18	130	12.300	1.420	50.4332	1
19	130	11.950	1.690	50.3835	1
20	130	12.350	1.990	50.1402	1
21	130	12.410	1.660	49.9327	1
22	130	12.270	1.380	50.5761	1
23	130	12.870	1.480	50.3878	1
24	130	12.400	1.950	50.0512	1
25	130	11.820	1.870	50.6620	1

Selected

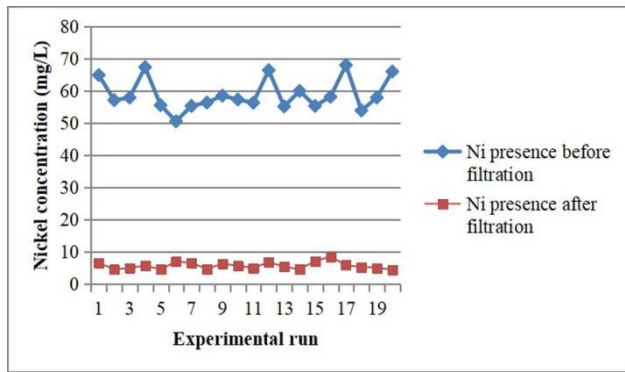


Figure 9 Experimental results of nickel presence before and after filtration.

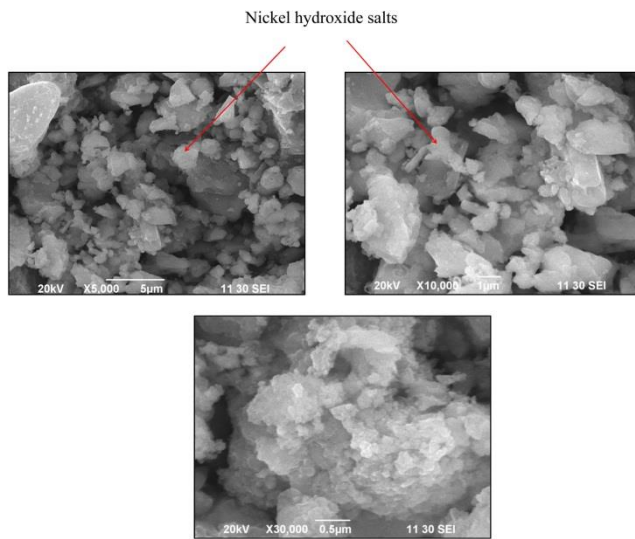


Figure 10 SEM image of adsorbents.

Figure 9 shows the experimental results show the nickel presence before and after the eco-friendly filtration. It can be noted that a significant amount of nickel content is adsorbed by these bio-adsorbents. SEM images of wood dust after filtration are shown in Figure 10 confirms the removal of nickel ions from the electrolyte. Nickel contents surfaced on the fibers are noted in these images.

The coconut shell powder contains high lignin and cellulose [35]. It was proved that lignin and holo-cellulose could adsorb nickel in water arrangement. In this manner, lignin and holo-cellulose were associated with nickel adsorption.

2.4. Optimization of ECM process parameters

Best machining conditions are intended to find out to get minimum Ni discharge. The regression Eqn. (1) is used for obtaining optimal cutting parameters. Optimization of ECM process parameters was done utilizing the steepest

Table 6. Limits of process and performance parameters

Variable	Goal	Lower	Upper	Weight	Weight	Importance
EC	In the range	130	190	1	1	3
V	In the range	11	15	1	1	3
U	In the range	1	3	1	1	3
Ni presence	Minimize	50.64	68.1	1	1	3

ascent (SA) method in combination with the desirability function (DF) approach. The response variable in this investigation is expressed as the equation given below [36] for tracing the best solution using SA -DF approach.

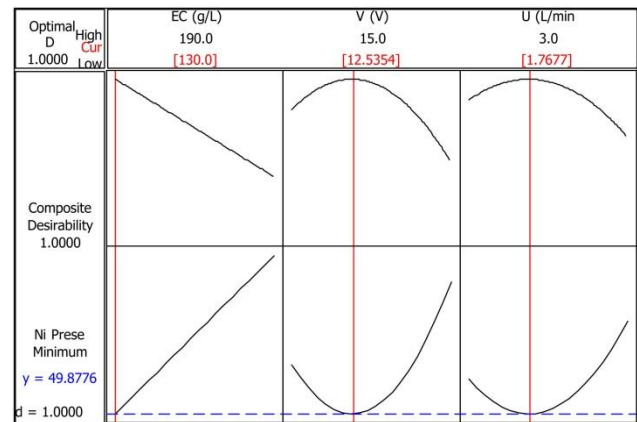


Figure 11 Response optimization plot.

The variables and response restrictions in Table 6 are used to apply the optimization tool. To see the outcomes of the optimization, look at Table 7 and Figure 11. In the following machining environment, the Ni discharge components are the lowest.

Voltage (V)	:12.535 V
Electrolyte concentration (EC)	:130 g/L
Flow rate (U)	:1.768 L/min
Ni presence	:49.8776 mg/L

3. Conclusion

In this paper, eco-friendly filtration of nickel hydroxide from the sludge during Electrochemical Machining of Monel 400 compound is presented. Natural environmental wastes such as coconut shell powder, wood dust powder, and bagasse were used as filtration material. The predominant ECM process parameters like applied voltage (V), flow rate (U), and electrolyte concentration (EC) were concentrated on the performance measures of material removal rate (MRR) and nickel content in the electrolyte previously also, after the filtration. The central composite design (CCD) of response surface methodology (RSM) is embraced for the experimentation. The lignin and holo-cellulose presence in the filtration material adsorb nickel hydroxide in the electrolyte solution. Its found to be the voltage of 12.535V, electrolyte concentration (EC) of 130 g/L and flow rate of 1.768 L/min discharges possible minimum nickel contents of 49.8776 mg/L into the electrolyte.

Table 7 Optimization results

Number	Solutions				
	EC	V	U	Ni presence	Desirability (Ni)
1	130	12.210	1.390	50.5976	1
2	130	12.490	1.370	50.5202	1
3	130	12.830	1.630	50.0980	1
4	130	12.890	1.440	50.5093	1
5	130	12.640	1.670	49.9318	1
6	130	12.160	1.720	50.0799	1
7	130	12.850	1.660	50.0892	1
8	130	12.220	1.990	50.2443	1
9	130	12.740	2.110	50.4790	1
10	130	13.090	1.780	50.3752	1
11	130	12.350	1.400	50.4749	1
12	130	12.860	1.490	50.3537	1
13	130	12.220	1.540	50.2202	1
14	130	12.890	1.960	50.2533	1
15	130	12.200	2.020	50.3274	1
16	130	12.535	1.768	49.8776	1
17	130	12.810	1.770	50.0023	1
18	130	12.300	1.420	50.4332	1
19	130	11.950	1.690	50.3835	1
20	130	12.350	1.990	50.1402	1
21	130	12.410	1.660	49.9327	1
22	130	12.270	1.380	50.5761	1
23	130	12.870	1.480	50.3878	1
24	130	12.400	1.950	50.0512	1
25	130	11.820	1.870	50.6620	1

Selected

Acknowledgment

The creators might want to thank appreciatively the TEQIP plan of the World Bank for financing the Atomic Absorption Spectroscopy equipment at the Government College of Technology, Coimbatore-641013, Tamilnadu, India.

References

- Ajmal M., Rao R.A., Ahmad R., and Ahmad J. (2000) Adsorption studies on Citrus reticulata (fruit peel of orange): removal and recovery of Ni(II) from electroplating wastewater. *Journal of Hazardous Materials*, **79**(1–2), 117–131.
- Ajmal M., Rao R.A.K., Anwar S., Ahmad J., and Ahmad R. (2003). Adsorption studies on rice husk: removal and recovery of Cd (II) from wastewater. *Bioresource Technology*, **86**, 147–149.
- Argun M.E., Dursun S., Ozdemir C., and Karatas M. (2007). Heavy metal adsorption by modified oak sawdust: thermodynamics and kinetics. *Journal of Hazardous Materials*, **141**(1), 77–85.
- Bhatnagar A., and Minocha A. (2010) Biosorption optimization of nickel removal from water using Punica granatum peel waste. *Colloids and Surfaces B: Bio interfaces*, **76**, 544–548.
- Burger M., Koll L., Werner E.A., and Platz A. (2012). Electrochemical machining characteristics and resulting surface quality of the nickel-base single-crystalline material LEK94. *Journal of Manufacturing Processes*, **14**, 62–70.
- Crini G. (2006). Non-conventional low-cost adsorbents for dye removal: a review. *Bioresource Technology*, **97**, 1061–1085.
- Curtis D.T., Soo S.L., Aspinwall D.K., and Sage C. (2009) Electrochemical superabrasive machining of a nickel-based aeroengine alloy using mounted grinding points. *CIRP Annals – Manufacturing Technology*, **58**, 173–176.
- Ewecharoen A., Thiravetyan P., and Nakbanpote W. (2008). Comparison of nickel adsorption from electroplating rinse water by coir pith and modified coir pith. *Chemical Engineering Journal*, **137**, 181–188.
- Gönen F., and Serin, D.S. (2012). Adsorption study on orange peel: Removal of Ni (II) ions from aqueous solution. *African Journal of Biotechnology*, **11**, 1250–1258.
- Kumar A., Balouch A., Pathan A.A., Abdulla, Jagirani M.S., Mahar A.M., Zubair M., and Laghari B. (2019). *Acta Chemica Malaysia (ACMY)*, **3**(1), 1–15.
- Kumar P.S., Ramalingam S., Kirupha S.D., Murugesan A., Vidhyadevi T., and Sivanesan S. (2011). Adsorption behavior of nickel (II) onto cashew nut shell: Equilibrium, thermodynamics, kinetics, mechanism and process design. *Chemical Engineering Journal*, **167**, 122–131.
- Malkoc E., and Nuhoglu Y. (2010). Nickel (II) adsorption mechanism from aqueous solution by a new adsorbent—Waste acorn of Quercus ithaburensis. *Environmental Progress & Sustainable Energy*, **29**, 297–306.
- Rajurkar K.P., Zhu D., McGeough J.A., Kozak J., and De Silva A. (1999). New developments in electro-chemical machining. *Annals of CIRP*, **48**(2), 567–579.
- Srivastava N.K., and Majumder C.B. (2008). Novel biofiltration methods for the treatment of heavy metals from industrial wastewater. *Journal of Hazardous Materials*, **151**(1), 1–8.
- Sudha R., Srinivasan K., and Premkumar P. (2015). Removal of nickel (II) from aqueous solution using Citrus Limettioides

- peel and seed carbon. *Ecotoxicology and Environmental Safety*, **117**, 115–123.
- Thevannan A., Mungroo R., and Niu C.H. (2010). Biosorption of nickel with barley straw. *Bioresource Technology*, **101**, 1776–1780.
- Tonshoff H.K., Egger R., and Klocke F. (1996). Environmental and safety aspects of electrophysical and electrochemical processes. *Annals of the CIRP*, **452**, 1–15.
- Watkins R.D., and Granoff B. (1992). Introduction to environmentally conscious manufacturing. *International Journal of Environmentally Conscious Manufacturing. MRS Bulletin*, **17**(3), 34–38.
- Xiaolei B., Yongbin Z., and Ningsong Q. (2020). Wire electrochemical micromachining of high-quality pure-nickel microstructures focusing on different machining indicators. *Precision Engineering*, **61**, 14–22.
- Xu Z., and Wang Y. (2019). Electrochemical machining of complex components of aero-engines: developments, trends, and technological advances. *Chinese Journal of Aeronautics*. doi: <https://doi.org/10.1016/j.cja.2019.09.016>.
- Yong Cheng G., Zengwei Z., and Dengyong W. (2017). Electrochemical Dissolution Behavior of the Nickel-Based Cast Superalloy K423A in NaNO₃ Solution. *Electrochimica Acta*, **253**, 379–389.
- Yong Cheng G., Zengwei Z., and Yongwei Z. (2019). Electrochemical deep grinding of cast nickel-base superalloys. *Journal of Manufacturing Processes*, **47**, 291–296.
- Zafar M.N., Aslam I., Nadeem R., Munir S., Rana U.A., Khan S.U.D. (2015). Characterization of chemically modified biosorbents from rice bran for biosorption of Ni (II). *Journal of the Taiwan Institute of Chemical Engineers*, **46**, 82–88.
- Zhang Y., Xu Z., Xing J., and Zhu D. (2016). Effect of tube-electrode inner diameter on electrochemical discharge machining of nickel-based super alloy. *Chinese Journal of Aeronautics*, **29**(4), 1103–1110.